
COMPUTATIONAL FLUID DYNAMICS: ITS CARBON FOOTPRINT AND ROLE IN CARBON EMISSION REDUCTION

Xiang I A Yang

Mechanical Engineering
Pennsylvania State University
State College, PA 16803
xzy48@psu.edu

Wen Zhang

Mechanics and Aerospace Engineering
Southern University of Science and Technology
Shenzhen 518055, China
zhangw6@sustech.edu.cn

Mahdi Abkar

Mechanical and Production Engineering
Aarhus University
Aarhus N 8200, Denmark
abkar@mpe.au.dk

William Anderson

Mechanical Engineering
University of Texas at Dallas
Richardson, TX, 75080
william.anderson@utdallas.edu

ABSTRACT

Turbulent flow physics regulates the aerodynamic properties of lifting surfaces, the thermodynamic efficiency of vapor power systems, and exchanges of natural and anthropogenic quantities between the atmosphere and ocean, to name just a few applications of contemporary importance. The space-time dynamics of turbulent flows are described via numerical integration of the non-linear Navier-Stokes equation – a procedure known as computational fluid dynamics (CFD). At the dawn of scientific computing in the late 1950s, it would be many decades before terms such as “carbon footprint” or “sustainability” entered the lexicon, and longer still before these themes attained national priority throughout advanced economies. The environmental cost associated with CFD is seldom considered. Yet, large-scale scientific computing relies on intensive cooling realized via external power generation that is primarily accomplished through the combustion of fossil fuels, which leads to carbon emissions. This paper introduces a framework designed to calculate the carbon footprint of CFD and its contribution to carbon emission reduction strategies. We will distinguish between “hero” and “routine” calculations, noting that the carbon footprint of hero calculations – which demand significant computing resources at top-tier data centers – is largely determined by the energy source mix utilized. We will also review CFD of flows where turbulence effects are modeled, thus reducing the degrees of freedom. Estimates of the carbon footprint are presented for such fully- and partially-resolved simulations as functions of turbulence activity and calculation year, demonstrating a reduction in carbon emissions by two to five orders of magnitude at practical conditions. Beyond analyzing CO₂ emissions, we quantify the benefits of applying CFD towards overall carbon emission reduction. The community’s effort to avoid redundant calculations via turbulence databases merits particular attention, with estimates indicating that a single database could potentially reduce CO₂ emissions by approximately O(1) million metric tons. Additionally, implementing CFD in the fluids industry has markedly decreased dependence on wind tunnel testing, which is anticipated to lead to CO₂ emission reduction.

1 Introduction

The concept of the carbon footprint has become central to assessing environmental impacts in the natural environment literature [1, 2]. Accurate carbon footprint quantification helps society understand the environmental impact of human activities and underpins strategies and policies to combat climate change [3]. Analyses of carbon footprints are now extensively available in scholarly literature. For example, Usman and Radulescu [4], along with others [5, 6], showed that renewable energy sources, while not entirely devoid of greenhouse gas emissions, significantly reduce carbon footprints compared to traditional fossil fuels. In urban development, the concept of “urban carbon footprints” focuses on greenhouse gas emissions from cities. Dodman (2009) highlighted that urban areas, although covering a small fraction of the Earth’s surface, contribute substantially to the global carbon footprint [7]. Kissinger et al. (2013) explored the material consumption aspects of urban carbon footprints [8]. Further work can be found in Refs. [9–11] but is not detailed here. In agriculture, Adom et al. (2012) reported greenhouse gas emissions from common dairy feeds in the United States (US) [12]. In public health, Okeke (2022) examined the impact of human carbon footprints, with an emphasis on Africa [13]. Furthermore, Kanemoto et al. [14], Ivanova et al. [15], Yang et al. [16], and Lomas et al. [17] estimated the carbon footprint mapping for the US, EU, China, and UK, providing spatial representation of carbon emissions and carbon sinks, taking factors like land use, international trades, supply chain, urbanization, and consumption patterns, into account.

This study examines the carbon footprints associated with computational simulations. Computational simulations serve as a crucial cornerstone in modern scientific research, enabling the exploration of complex phenomena across diverse fields such as physics, engineering, biology, and environmental science. By mimicking the behaviors of systems under various conditions, simulations offer invaluable insights into processes that are otherwise too challenging to observe directly, significantly reducing the time, cost, and ethical issues associated with traditional experiments. Here, we focus on computational fluid dynamics (CFD). CFD concerns the simulation and analysis of fluid flow, heat transfer, and related phenomena. By solving the Navier-Stokes equations numerically, CFD enables the prediction of fluid behavior in complex systems without the need for physical prototypes, reducing both cost and development time.

Recent advancements in high-performance computing (HPC), including petascale and exascale systems have significantly enhanced the accessibility of CFD [18, 19]. Tools like large-eddy simulation (LES) have gained widespread application in industries like wind energy [20–22], notably in validating wind farm models [23, 24] and studying the interaction of wind turbines with the atmosphere [25–27]. Additionally, LES has been instrumental in urban environment studies [28] and in aerodynamics, particularly in the development of the “certificate by analysis” (CbA) concept [29], which seeks to replace part and even all of wind tunnel tests with CFD simulations. In this context, researchers such as Lehmkuhl et al. [30], and others [31–33], have successfully validated their CFD calculations against experimental drag and lift data. The application of CFD extends beyond these areas to include turbomachinery [34–36], underwater hydrodynamics [37–39], and many other fields [40]. Such widespread use of CFD leads to significant energy consumption and therefore a carbon footprint. This paper estimates the carbon footprint of CFD and assesses CFD’s role in mitigating carbon emissions.

The rest of the paper is organized as follows. The methodology is summarized in Sec. 2. The results and our discussion are presented in Sec. 3. Finally, we conclude in Sec. 4.

2 Methods

The execution of CFD calculations relies on HPC centers, through which CFD has a carbon footprint. In this study, we focus on the carbon footprint during the execution of CFD only, and by adapting the method outlined in Ref. [41], the carbon footprint of a CFD calculation is given by

$$\text{Carbon footprint} = \text{Energy consumption} \times \text{Carbon intensity}. \quad (1)$$

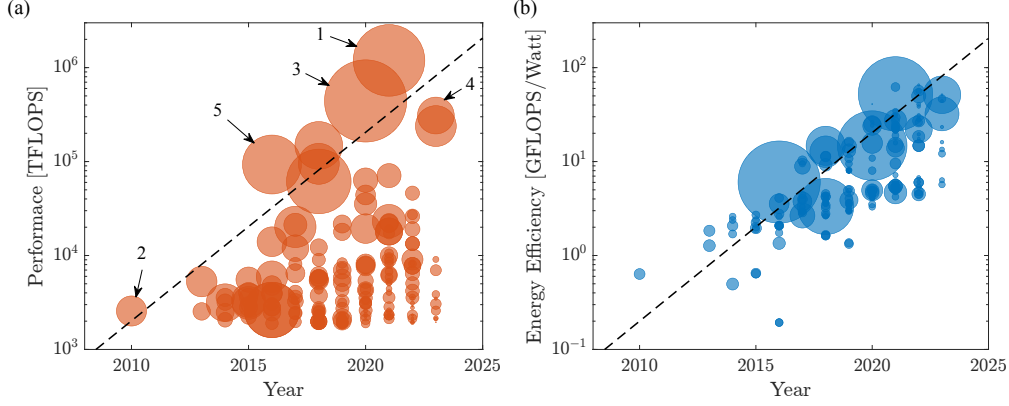


Figure 1: (a) Performance in FLOPS of the top 500 HPC systems [47]. The circles represent the HPC systems. Their sizes represent the total power usage. (b) Energy efficiency in GFLOPS/Watt of the top 500 HPC systems [47]. The sizes of the circles represent the total core numbers of the centers. The dashed lines represent the doubling time of 1.5 years. The highlighted HPC systems are: 1. Frontier, 2. Tianhe-1A, 3. Supercomputer Fugaku, 4. Lumi, 5. Sunway Taihu-Light.

Matthews et al. (2008) [42], along with others [43–45], emphasized the importance of life-cycle analysis (LCA) for a holistic view encompassing the entire product life cycle. However, LCA’s complexity warrants separate, future investigation.

Equation 1 contains two terms. The energy consumption term is

$$\text{Energy Consumption} = \text{Run time} \times \text{PSF} \times \text{IT power usage} \times \text{PUE}. \quad (2)$$

Here, “run time” is the duration of a CFD calculation. “PSF” is the pragmatic scaling factor. In the context here, PSF accounts for small-scale test runs. For proficient CFD practitioners conducting large-scale CFD on high-end HPC clusters, the value of PSF would be very close to 1. “IT power usage” is defined as

$$\text{IT power usage} = \frac{\text{Performance}}{\text{Energy efficiency}}. \quad (3)$$

“Performance” is measured in floating-point operations per second (FLOPS), and energy efficiency in floating-point operations per Joule or FLOPS/Watt. The peak performance and the energy efficiency of the top 500 HPC systems are displayed in Fig. 1. “Frontier”, which was put into service in 2021, is a top-tier HPC system. It has a peak performance of 10^6 TFLOPS and an energy efficiency of 52.59 GFLOPS/Watt. Here, 1 TFLOPS is 10^{12} floating-point operations per second, and 1 GFLOPS is 10^9 floating-point operations per second. “Tianhe-1A” is a low-tier HPC system (by today’s standard). Its performance is 2.5×10^3 TFLOPS, and its energy efficiency is 0.64 GFLOPS/Watt. The “Mira” system, utilized for the $Re_\tau = 5200$ channel flow DNS in 2013 [46], has a power usage of 3,945 kilowatts. It was once a top contender but is now off the list, due to the rapid development of HPC. The data in Fig. 1 suggests that the performance and the energy efficiency of top-tier HPC systems have been doubling every one and a half years or so, following Moore’s law. The performance of the lower-tier systems, on the other hand, has stayed at 2×10^3 TFLOPS since 2010, with their energy efficiency increasing annually.

PUE or “power usage effectiveness” was a concept proposed by Malone and Belady [48, 49]. It measures the total energy needed to operate a data center and is defined as:

$$\text{PUE} = \frac{\text{Facility Power Usage}}{\text{IT Power Usage}}. \quad (4)$$

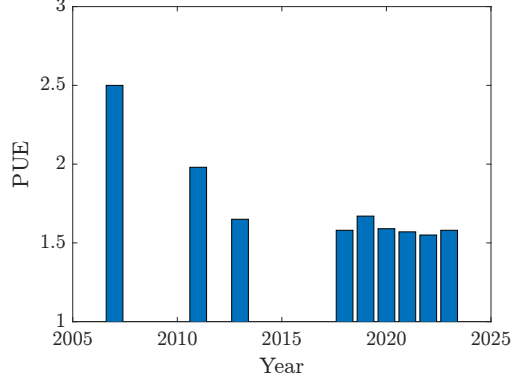


Figure 2: Annualized PUE from 2007 to 2023 [53].

The value of PUE depends on the IT equipment, the cooling system, the location, the climate, the size, and the design of the data center [50]. A 2006 study of 22 US data centers reported PUE values between 1.33 and 3, averaging 2.04 [51]. A subsequent 2011 survey of 115 data centers, with 70 responses, indicated an average PUE of 1.69 [52]. Figure 2 charts the evolution of the average PUE from 9 surveys conducted between 2006 and 2023 [53]. The data suggests that the PUE value has stabilized at 1.5-1.7 since 2018. Although more center-specific data is not available, the average value of PUE= 1.69 suffices for the scope of this study.

The carbon intensity (CI), quantifies the CO₂ emissions per unit of energy produced. Expressed in grams of CO₂ per kilowatt-hour (kWh), it is calculated as follows:

$$CI = \sum_i p_i CI_i. \quad (5)$$

Here, CI represents the aggregated carbon intensity, p_i denotes the fraction of the i th energy source in the overall mix, and CI_i is the carbon intensity of that specific energy source. The composition of energy sources in the US from 1950 to 2022 is displayed in Fig. 3. Initially, coal, natural gas, and renewables were predominant until the 1980s, when nuclear power emerged as a significant contributor [54]. A notable shift is observed in the fraction of renewables, decreasing from 28.9% in 1950 to 8.3% in 2007, overshadowed by the rapid expansion of other energy forms. Additionally, coal's share in the energy mix plummeted from 55.9% in 1985 to 23.1% in 2020. The carbon intensities of the primary energy sources and the aggregated carbon intensity are displayed in Fig. 4. The carbon intensities of nuclear and renewable sources are relatively low, under 50 gCO₂/kWh, and are negligible compared to those of coal and natural gas. The carbon intensity of coal has remained around 1000 gCO₂/kWh, and natural gas at 400 gCO₂/kWh. The overall carbon intensity has been on a steady decline, as indicated by the data. This reduction can be largely attributed to the decreasing reliance on coal and natural gas for electricity generation.

Combining Eqs. 1, 2, 3, and 5, we have the following estimate for the carbon footprint:

$$\text{Carbon footprint} \approx \text{Run time} \times \frac{\text{Performance}}{\text{Energy efficiency}} \times \text{PUE} \times \text{PSF} \times (p_{\text{coal}} CI_{\text{coal}} + p_{\text{natural gas}} CI_{\text{natural gas}}). \quad (6)$$

Here, we have neglected the emissions from nuclear and renewable energies. Based on the discussions in this section, PSF is 1, and PUE is 1.7. The carbon intensities of coal and natural gas have remained relatively stable since 2005 at 1000 gCO₂/kWh and 400 gCO₂/kWh, respectively.

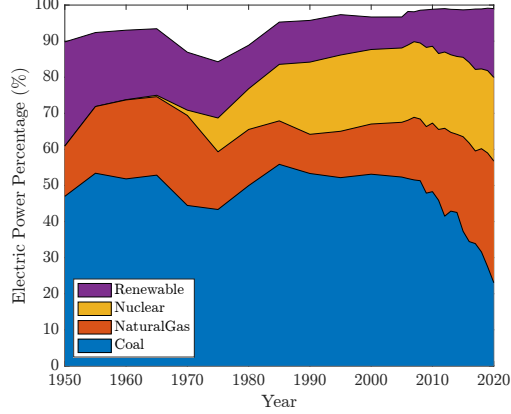


Figure 3: Composition of the energy sources in the US [54].

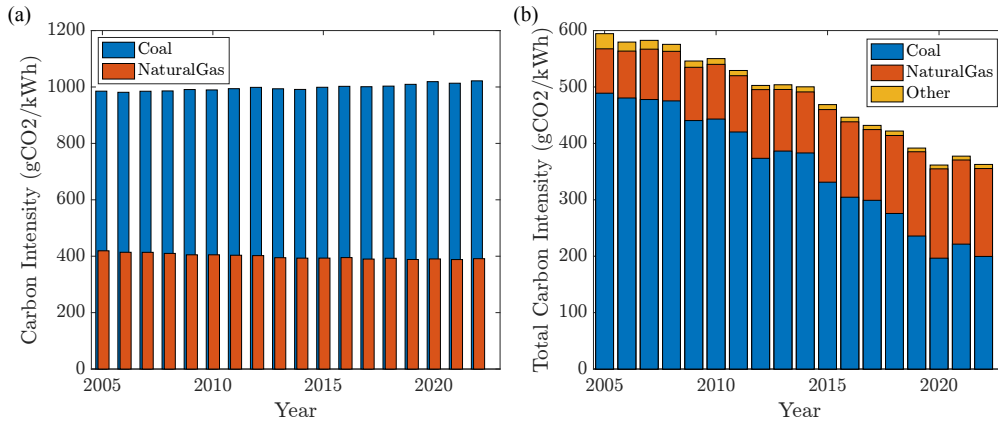


Figure 4: (a) Carbon intensity of coal and natural gas in the US [54]. (b) Composition of the aggregated carbon intensity in the US [55].

3 Results and discussion

3.1 Hero and routine calculations

We differentiate between “hero” and “routine” calculations. A hero calculation is done on a top-tier HPC system, utilizing a substantial portion of its cores for a stipulated period of time (stipulated by the data center). For these top-tier HPC systems, both the performance and the energy efficiency double approximately every 1.5 years. As a result, the performance-to-energy efficiency ratio remains approximately constant year-on-year, at around 10 MW. It then follows from Eq. 6 that the carbon footprint of a hero calculation is:

$$\text{Carbon footprint (kg CO}_2) \approx 1.7 \times 10^4 \times \text{Run time (h)} \times (p_{\text{coal}} + 0.4p_{\text{natural gas}}), \quad (7)$$

where the run time usually does not exceed a couple of hundred hours, and p_{coal} and $p_{\text{natural gas}}$ are the fraction of coal and natural gas in the mix of the energy sources. This estimate tends to be on the higher side, assuming full cluster utilization. While not included here, an equivalent run time could adjust for this overestimation. Equation 7 implies that the carbon footprint of a hero calculation largely depends on the energy source mix. As the US shifts away from coal, the carbon footprint of such calculations is set to decrease. Conversely, for a routine calculation on a low-tier HPC system, the run time can range from a few hours to a year, depending on the task and the availability of the resources. For low-tier, performance has stabilized at about 2×10^3 TFLOPS since 2010, and the energy efficiency doubles every

Year	Re_τ	Domain	Grid	Cores	Wall time (h)	Region	Reference
1987	180	$4\pi h \times 2h \times 2\pi h$	$192 \times 129 \times 160$	4	62.5	USA	Kim et al. [66]
1999	590	$2\pi h \times 2h \times \pi h$	$384 \times 257 \times 384$	N/A	N/A	USA	Moser et al. [67]
2004	950	$8\pi h \times 2h \times 3\pi h$	$3072 \times 385 \times 2304$	N/A	N/A	Spain/USA	del Alamo et al. [68]
2006	2k	$8\pi h \times 2h \times 3\pi h$	$6144 \times 633 \times 4608$	2048	2929	Spain	Hoyas & Jimenez [69]
2013	5.2k	$8\pi h \times 2h \times 3\pi h$	$10240 \times 1536 \times 7680$	524288	496	USA	Lee et al. [46, 70]
2014	4k	$6\pi h \times 2h \times 2\pi h$	$8192 \times 1024 \times 4096$	N/A	N/A	Germany	Bernardini et al. [71]
2014	4.2k	$2\pi h \times 2h \times \pi h$	$2048 \times 1081 \times 2048$	N/A	N/A	Spain	Lozano & Jimenez [72]
2018	8k	$16h \times 2h \times 6.4h$	$8640 \times 4096 \times 6144$	N/A	N/A	Japan	Yamamoto & Tsuji [73]

Table 1: Details of some hero channel flow DNSs. N/A is “not available”.

1.5 years or so. Thus, Eq. 6 gives the following estimates for the carbon footprint of a routine CFD calculation:

$$\text{Carbon footprint (kg CO}_2) \approx 6.6 \times 10^3 \times \text{Run time (h)} \times (p_{\text{coal}} + 0.4p_{\text{natural gas}}) \times 2^{-\frac{\text{Year} - 2010}{1.5}}, \quad (8)$$

where we have baselined against Tianhe-1A established in 2010. This too is an overestimate, assuming full cluster utilization. Aside from the energy source composition, the increase in energy efficiency will also contribute to the decrease of the carbon footprint.

3.2 Direct numerical simulation

Direct numerical simulation (DNS) provides accurate solutions to the Navier-Stokes. These solutions have yielded significant insights into flow physics, leading to the development of concepts such as the inner cycle [56], turbulence islands [57], and the momentum cascade [58, 59]. Furthermore, DNS has been instrumental in validating models and theories, including the attached eddy model [60–62] and wall models [63–65]. Consider, e.g., direct numerical simulation (DNS) of channel flow, a canonical configuration in fluid dynamics. DNS of this flow dates back to 1987. The calculation was at a friction Reynolds number of $Re_\tau = 180$ in a domain sized $4\pi \times 2 \times 2\pi$ [66]. Subsequently, DNSs of channel flow at increasingly higher Reynolds numbers have been performed on progressively more powerful HPC systems. Table 1 summarizes some of the hero calculations, including their Reynolds numbers, computation times, HPC systems used, and domain and grid sizes.

Figure 5 illustrates the sizes of the DNS calculations in terms of grid points. Here, we compile data for DNSs as well as LES published in the Journal of Fluid Mechanics. The figure contains the hero calculation data in Table 1, and routine calculations as well. The size of the hero calculations has escalated from fewer than 10^7 grid points in 1987 [66] to over 10^{11} in 2015 [46], yet there has not been a significant increase since. The sizes of routine calculations, on the other hand, range from 10^6 to the size of the hero calculation of the time for DNS and from 10^5 to the size of the hero calculation of the time for LES. In these two figures, we have indicated the expected growth if the CFD community had kept pace with HPC developments, i.e., running the same DNS and LES codes on the top machines. The trend, shown in Fig. 5, is somewhat disheartening. It appears the CFD community has not continued to invest in hero calculations at the rate of HPC developments.

We now present a case study and estimate the carbon footprint of the channel DNS in Ref. [46]. This simulation was performed on the “Mira” HPC system. The calculation utilized 524k cores out of the 768k cores in the system and lasted for 500 hours—it is one of the largest CFD calculations to date. In the year 2013, the fraction of coal and natural gas in the mix of the energy sources are 42.9% and 21.8%. It follows from Eq. 6 that the carbon footprint of this DNS calculation is:

$$\text{Carbon footprint} \approx 500 \text{ h} \times 4 \text{ MW} \times \frac{524}{768} \times 1.69 \times 1 \times (42.9\% + 0.4 \times 21.8\%) \text{ kg CO}_2/\text{kWh} \approx 10^6 \text{ kgCO}_2. \quad (9)$$

To contextualize this figure, the carbon footprint of a Boeing 777 flight from New York to Beijing and back is approximately 1.4×10^6 kgCO₂, assuming 3600 kg CO₂ emission per passenger and 388 passengers on the plane [74].

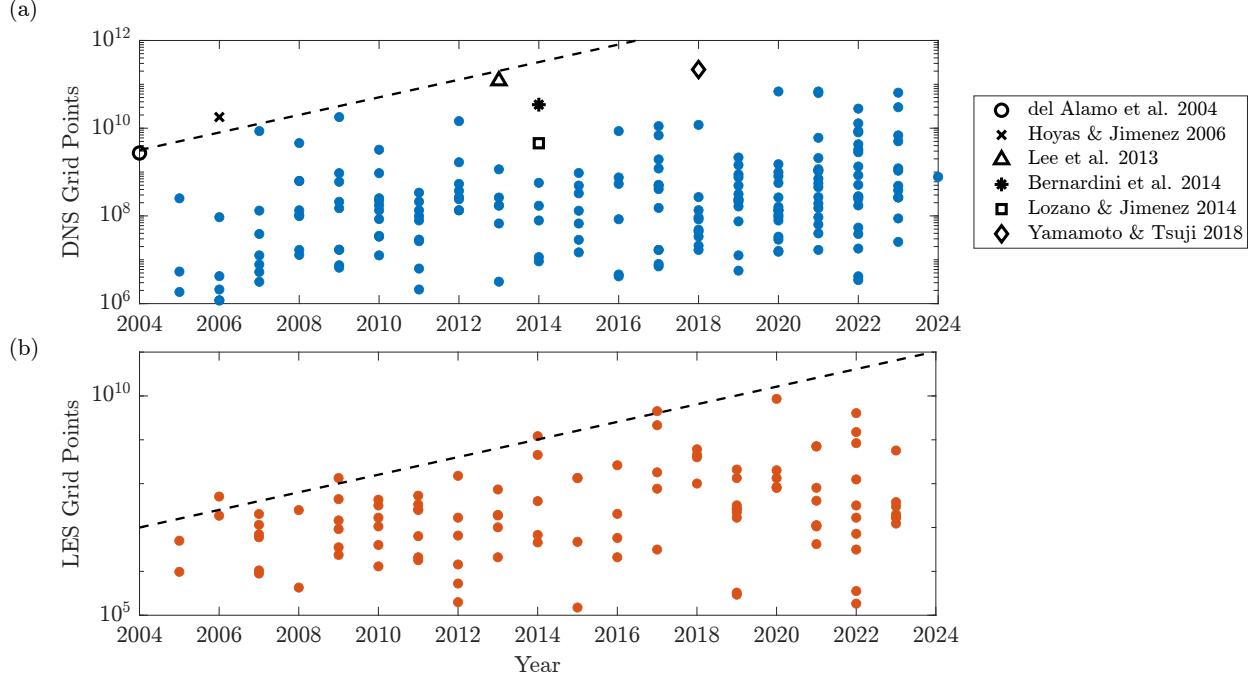


Figure 5: (a) The number of grid points in DNSs. (b) The number of grid points in LESs. The hero calculations in Table 1 are highlighted. The dots are DNS and LES reported in the Journal of Fluid Mechanics. The references used to generate the figure are detailed in the Appendix. This is not meant to be comprehensive. The dashed lines represent a doubling time of 1.5 years.

Before we proceed, we make a remark. It is common that a paper elaborates on the numerics and the setup but says nothing about the actual computation, including the computing time and the cluster used. This shows a lack of awareness of the issue of carbon footprint. A goal of this work is to help bring this aspect of CFD to the reader’s attention.

Although it is hard to get direct estimates for carbon emissions due to a lack of information, indirect estimates are viable. Here, we provide such estimates as a function of the Reynolds number and the year of calculation. We will assume constant carbon intensity and resource utilization efficiency. Errors due to these assumptions are not to exceed a factor of 2—considering the rapid annual increase of energy efficiency and FLOP counts, such errors are acceptable. Utilizing Eq. 6, we have

$$\text{Carbon footprint} \approx \text{Carbon footprint}_{\text{baseline}} \times \frac{\text{FLOP counts}}{\text{FLOP counts}_{\text{baseline}}} \frac{\text{Energy efficiency}_{\text{baseline}}}{\text{Energy efficiency}}. \quad (10)$$

That is, the carbon footprint of a calculation is proportional to the FLOP counts and inversely proportional to the energy efficiency. The FLOP count scales as Re_τ^4 for DNS of channel flow, assuming fixed domain size, grid resolution, the Courant–Friedrichs–Lewy number [75]:

$$\frac{\text{FLOP counts}}{\text{FLOP counts}_{\text{baseline}}} = \left(\frac{Re_\tau}{Re_{\tau,\text{baseline}}} \right)^4. \quad (11)$$

The energy efficiency ratio is

$$\frac{\text{Energy efficiency}_{\text{baseline}}}{\text{Energy efficiency}} = 2^{-\frac{\text{Year} - \text{Baseline Year}}{1.5}}, \quad (12)$$

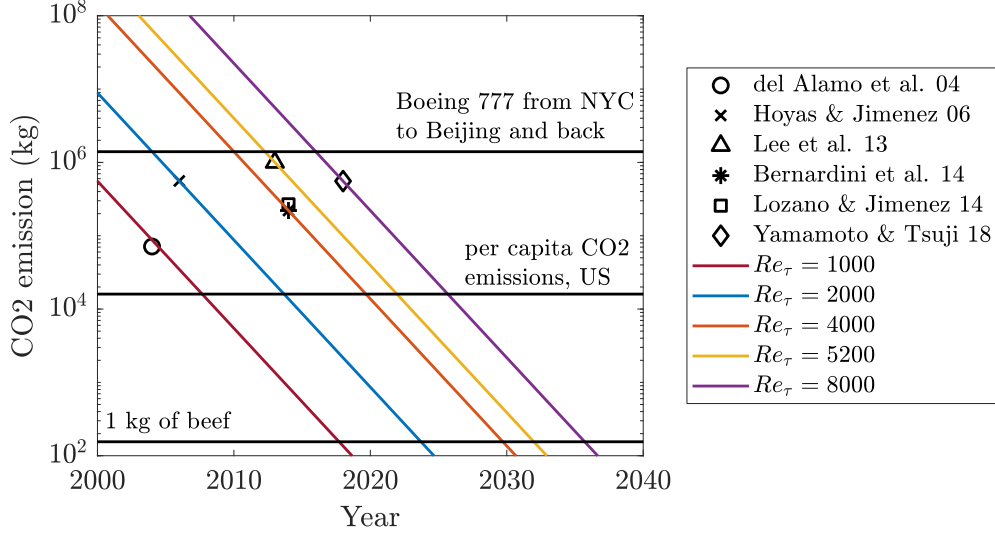


Figure 6: Estimates of carbon footprint for channel flow DNS according to Eq. 13.

per Moore’s law. By taking the $Re_\tau = 5200$ channel flow calculation as our baseline, the above equations yield

$$\text{Carbon footprint (kg CO}_2) \approx 10^6 \times \left(\frac{Re_\tau}{5200} \right)^4 \times 2^{-\frac{\text{Year} - 2013}{1.5}}. \quad (13)$$

Figure 6 illustrates the carbon footprint of channel flow DNS calculations at varying Re_τ values, from 1000 to 8000, between year 2000 to year 2040. To provide context, we indicate the carbon emission of serving 1 kg of beef [76], the per capita CO2 emission in the US in the year 2022 [77], as well as the emissions from a Boeing 777 flight from New York to Beijing and back [74]. From Fig. 6, we see that the carbon footprint escalates significantly with the Reynolds number. For instance, a $Re_\tau = 1000$ channel flow calculation today emits less CO2 than producing 1 kg of beef, whereas a $Re_\tau = 8000$ calculation’s emissions are on par with those of a round-trip Boeing 777 flight from New York to Beijing. Nonetheless, for a given Reynolds number, the carbon footprint decreases annually, thanks to the increasing energy efficiency. For example, repeating the $Re_\tau = 5200$ channel flow DNS in 2025 would result in a carbon footprint of 10^4 kg CO2. Lastly, examining “hero” calculations from 2000 to 2020, we observe a plateau and a slight decrease in the carbon footprint. This is consistent with the results in Fig. 5—the CFD community has not kept up with the developments of HPC.

3.3 Turbulence modeling

DNS is prohibitively expensive for flows at practically relevant Reynolds numbers due to the necessity of resolving all scales within the flow. To make CFD practical, one approach is to model the small scales and the flow within the wall layer. This gives rise to wall-resolved LES (WRLES) and wall-modeled LES (WMLES).

In this subsection, we explore the benefits of turbulence modeling through the lens of carbon emissions reduction. While current literature on LES lacks the data to directly estimate the carbon footprint, indirect estimation methods are feasible. We employ Equation 10 for this purpose. The energy efficiency ratio is determined by Eq. 12, and we assume that the ratio of floating-point operation (FLOP) counts mirrors the computational cost ratio. To further simplify, we assume the computational cost directly correlates with grid size. This implies equivalent time steps for LES and DNS, which is a crude approximation.

According to analyses in Refs. [75, 78], we derive the following FLOP count ratios:

$$\frac{Re_{L_x} = 3.5e7 \text{ BL DNS}}{Re_\tau = 5200 \text{ channel DNS}} \approx 1, \quad (14)$$

and

$$\begin{aligned} \frac{Re_{L_x} \text{ BL DNS}}{Re_{L_x} = 3.5e7 \text{ BL DNS}} &\approx \left(\frac{Re_{L_x}}{3.5e7}\right)^{2.05}, \\ \frac{Re_{L_x} \text{ BL WRLES}}{Re_{L_x} = 3.5e7 \text{ BL DNS}} &\approx 0.68 \frac{Re_{L_x}^{1.86}}{(3.5e7)^{2.05}}, \\ \frac{Re_{L_x} \text{ BL WRLES}}{Re_{L_x} = 3.5e7 \text{ BL DNS}} &\approx 7.6e4 \frac{Re_{L_x}^{1.00}}{(3.5e7)^{2.05}}. \end{aligned} \quad (15)$$

These ratios, and hence the subsequent analysis, rest on the assumptions delineated in Ref. [78]. From Eqs. 10, 12, 14, and 15, we infer the carbon footprints for boundary layer DNS, WRLES, and WMLES as follows:

$$\text{Carbon footprint of boundary layer DNS (kg CO}_2) \approx 10^6 \times \left(\frac{Re_{L_x}}{3.5e7}\right)^{2.05} \times 2^{-\frac{\text{Year} - 2013}{1.5}}, \quad (16)$$

$$\text{Carbon footprint of boundary layer WRLES (kg CO}_2) \approx 7 \times 10^5 \times \frac{Re_{L_x}^{1.86}}{(3.5e7)^{2.05}} \times 2^{-\frac{\text{Year} - 2013}{1.5}}, \quad (17)$$

and

$$\text{Carbon footprint of boundary layer WMLES (kg CO}_2) \approx 10^{11} \times \frac{Re_{L_x}^1}{(3.5e7)^{2.05}} \times 2^{-\frac{\text{Year} - 2013}{1.5}}. \quad (18)$$

Here, we have assumed identical efficiency for LES and DNS codes and omitted the costs related to sub-grid scale and wall models. These assumptions likely make our estimates conservative. Further refinement of these estimates is challenging and is deferred to future research. For boundary layers at a Reynolds number of $Re_{L_x} = 10^9$, typical for underwater vehicles, our calculations yield carbon footprint estimates for DNS, WRLES, and WMLES in 2023 of 10^7 , 10^5 , and 3×10^2 kg, respectively. These figures starkly illustrate that DNS at such Reynolds numbers is impractical, WRLES, which models the sub-grid scale motions, is feasible but with significant carbon emissions, and WMLES, which models both the sub-grid scale motions and the near-wall flows, offers a viable and environmentally sustainable option.

3.4 Turbulence Database

High-fidelity CFD simulations, known for their computational intensity, necessitate significant resources and result in notable carbon emissions. To mitigate these demands, various online repositories have been established, hosting extensive datasets from simulations. Here, we take the Johns Hopkins Turbulence Database (JHTDB) as an example [79, 80]. The database offers DNS data on isotropic turbulence, magneto-hydrodynamic turbulence, channel flow, and boundary layer flows, encompassing over 300 Terabytes of data [81]. To date, the database has received 4×10^{14} point queries. The carbon footprint of the CFD solution at a grid point is not straightforward to accurately estimate, as it involves flow condition, the cluster of the calculation, and the time of the calculation, among others. Nonetheless, an approximate figure can be drawn from the analyses of the $Re_\tau = 5200$ channel flow DNS, i.e., our baseline case. Per the estimate there, generating CFD solution at one grid point leads to a carbon emission of 8.3×10^{-3} g CO₂. Considering that the power needed to operate the database is negligible compared to that needed for CFD calculation, JHTDB alone has contributed to a 3.3 million metric tons CO₂ reduction in carbon emission.

3.5 Aviation

In the field of aviation, CFD has emerged as a standard tool alongside wind tunnel. Its use in the process of design, analysis, certification, and maintenance has facilitated progress in both internal and external flows [82, 83] reducing the reliance on physical wind tunnel testing and at the same time accelerating the development cycles of aircraft. Johnson et al. (2005) highlighted a significant reduction in the number of wind tunnel tests for aircraft wings at Boeing, from 77 in the late 1970s to just 10 by the late 1990s [84], i.e., a reduction of 87%. This shift diminished the need for extensive wind tunnel hours, through which CFD helps reduce carbon emissions [85]. Take the Boeing 747 as an example. Its development in the 60s and the 70s relied primarily on wind tunnel experiments. The wind tunnel hours were about 10,000 [86]. The power of the fan in the Boeing low-speed aero acoustic facility is 7 MW [87]. It follows that the energy consumption of wind tunnel tests is $O(10^8)$ kWh. It is not fair to compute energy saving according to $87\% \times O(10^8)$ kWh, and it is difficult to estimate the reduction in carbon emission, but it is safe to claim the potential of CFD in reducing the carbon footprint of aircraft design.

CFD is also set to play a critical role in mitigating the aviation industry’s carbon footprint. Without advancements in technology, CO₂ emissions from domestic and international aviation are projected to reach 450 million metric tons by 2050 [88]. The goal, as outlined in the US Aviation Climate Action Plan, is to stabilize carbon emissions at the 2019 level of approximately 210 million metric tons [88], thus creating a reduction target of 240 million metric tons. Biofuels derived from saturated fatty acids are expected to address about half of this gap [89, 90]. Operational improvements contribute a very small portion. The renewal of air fleets with newer, more efficient aircraft is anticipated to account for the remainder of the reduction, a process that is significantly influenced by the application of CFD in aircraft design and development.

4 Conclusions

We propose a framework for estimating the carbon footprint of computational simulations, incorporating factors such as runtime, performance, energy efficiency, power usage effectiveness (PUE), scaling efficacy, energy mix, and the carbon intensity of each energy source. We delineate here from routine calculations, noting that the carbon footprint of the former is directly linked to carbon intensity. As the United States moves away from coal, a reduction in the environmental impact of these calculations is anticipated. Conversely, the carbon footprint of routine calculations is influenced by both carbon intensity and energy efficiency, which are improving rapidly.

A case study on the $Re_\tau = 5200$ channel flow DNS reveals an estimated carbon footprint of 10^6 kg CO₂, equivalent to emissions from a round-trip Boeing 777 flight between New York and Beijing. Based on this data, we derive formulas for estimating the carbon footprints of different types of DNS and LES, showing significant benefits of turbulence modeling. These formulas will allow CFD practitioners to estimate the environmental impacts of their calculations as a function of the Reynolds number and the year—before or after the calculation.

The paper also highlights the CFD community’s efforts in carbon emission reduction, such as the Johns Hopkins Turbulence Database (JHTDB), which has saved approximately 3.3 million metric tons of carbon emissions by eliminating redundant calculations. Moreover, CFD’s role in minimizing wind tunnel tests has notably reduced carbon emissions.

Last but not least, we call for a balanced view. Take CFD as an example, while it generates carbon emissions, CFD has also contributed to the reduction of carbon emissions—both sides must be considered when assessing the environmental impact.

Acknowledgement

This work was presented at the Flow, Turbulence, and Wind Energy Symposium. The authors acknowledge inputs from the participants.

A Supporting material for Fig. 5

References used to generate Fig. 5.

References

- [1] T. Wiedmann and J. Minx, "A definition of 'carbon footprint'," *Ecological Economics Research Trends*, vol. 1, no. 2008, pp. 1–11, 2008.
- [2] K. Protocol, "Kyoto protocol," *UNFCCC Website. Available online: http://unfccc.int/kyoto_protocol/items/2830.php (accessed on 1 January 2011)*, 1997.
- [3] E. G. Hertwich and G. P. Peters, "Carbon footprint of nations: a global, trade-linked analysis," *Environ. Sci. Tech.*, vol. 43, no. 16, pp. 6414–6420, 2009.
- [4] M. Usman and M. Radulescu, "Examining the role of nuclear and renew. energ. in reducing carbon footprint: does the role of technological innovation really create some difference?," *Sci. Total Environ.*, vol. 841, p. 156662, 2022.
- [5] C. Kelly, N. C. Onat, and O. Tatari, "Water and carbon footprint reduction potential of renew. energ. in the united states: A policy analysis using system dynamics," *J. Clean. Prod.*, vol. 228, pp. 910–926, 2019.
- [6] P. Arévalo, A. Cano, and F. Jurado, "Mitigation of carbon footprint with 100% renew. energ. system by 2050: The case of galapagos islands," *Energy*, vol. 245, p. 123247, 2022.
- [7] D. Dodman, "Urban density and climate change." <http://www.unfpa.org/webdav/site/global/users/schensul/public/ccpd/papers/dodman%20paper.pdf>.
- [8] M. Kissinger, C. Sussman, J. Moore, and W. E. Rees, "Accounting for the ecological footprint of materials in consumer goods at the urban scale," *Sustainability*, vol. 5, no. 5, pp. 1960–1973, 2013.
- [9] J. Lin, Y. Hu, S. Cui, J. Kang, and A. Ramaswami, "Tracking urban carbon footprints from production and consumption perspectives," *Environ. Res. Lett.*, vol. 10, no. 5, p. 054001, 2015.
- [10] J. Fan, X. Guo, D. Marinova, Y. Wu, and D. Zhao, "Embedded carbon footprint of chinese urban households: structure and changes," *J. Clean. Prod.*, vol. 33, pp. 50–59, 2012.
- [11] R. Koide, S. Kojima, K. Nansai, M. Lettenmeier, K. Asakawa, C. Liu, and S. Murakami, "Exploring carbon footprint reduction pathways through urban lifestyle changes: a practical approach applied to japanese cities," *Environ. Res. Lett.*, vol. 16, no. 8, p. 084001, 2021.
- [12] F. Adom, A. Maes, C. Workman, Z. Clayton-Nierderman, G. Thoma, and D. Shonnard, "Regional carbon footprint analysis of dairy feeds for milk production in the usa," *Int. J. Life Cycle Assess.*, vol. 17, pp. 520–534, 2012.
- [13] G. Okeke, "Carbon footprints & global climate change in relationship to pulic health & local economic effects," *Op. J. Environ. Res. (ISSN: 2734-2085)*, vol. 3, no. 2, pp. 65–76, 2022.
- [14] K. Kanemoto, D. Moran, and E. G. Hertwich, "Mapping the carbon footprint of nations," *Environ. Sci. Tech.*, vol. 50, no. 19, pp. 10512–10517, 2016.
- [15] D. Ivanova, G. Vita, K. Steen-Olsen, K. Stadler, P. C. Melo, R. Wood, and E. G. Hertwich, "Mapping the carbon footprint of eu regions," *Environ. Res. Lett.*, vol. 12, no. 5, p. 054013, 2017.

Table 2: References used for the data points in Figure 1 (Part 1/3)

Year	Max Grid Points	DOI	Type	Year	Max Grid Points	DOI	Type
2024	774400000	10.1017/jfm.2023.1099	DNS	2020	805306368	10.1017/jfm.2019.1012	DNS
2023	1073741824	10.1017/jfm.2023.971	DNS	2020	160168320	10.1017/jfm.2020.601	DNS
2023	6865551360	10.1017/jfm.2023.104	DNS	2020	33554432	10.1017/jfm.2020.402	DNS
2023	5033164800	10.1017/jfm.2023.26	DNS	2020	563871744	10.1017/jfm.2020.173	DNS
2023	30064771072	10.1017/jfm.2023.764	DNS	2020	78643200	10.1017/jfm.2020.33	DNS
2023	25600000	10.1017/jfm.2023.884	DNS	2020	28794880	10.1017/jfm.2020.452	DNS
2023	382205952	10.1017/jfm.2023.728	DNS	2020	989148160	10.1017/jfm.2020.669	DNS
2023	485587656	10.1017/jfm.2022.1056	DNS	2020	94371840	10.1017/jfm.2020.874	DNS
2023	64424509440	10.1017/jfm.2022.1013	DNS	2020	68719476736	10.1017/jfm.2020.146	DNS
2023	87512161	10.1017/jfm.2023.502	DNS	2020	15271410	10.1017/jfm.2020.629	DNS
2023	1212678144	10.1017/jfm.2023.359	DNS	2020	15884544	10.1017/jfm.2020.590	DNS
2023	263831040	10.1017/jfm.2023.870	DNS	2020	1509949440	10.1017/jfm.2020.488	DNS
2023	262144000	10.1017/jfm.2023.307	DNS	2020	263831040	10.1017/jfm.2020.412	DNS
2022	843750000	10.1017/jfm.2022.764	DNS	2020	134217728	10.1017/jfm.2020.218	DNS
2022	1337720832	10.1017/jfm.2022.559	DNS	2020	134217728	10.1017/jfm.2020.162	DNS
2022	54000000	10.1017/jfm.2022.22	DNS	2020	106168320	10.1017/jfm.2020.780	DNS
2022	8589934592	10.1017/jfm.2022.434	DNS	2019	5640192	10.1017/jfm.2019.482	DNS
2022	18000000	10.1017/jfm.2022.822	DNS	2019	1440000000	10.1017/jfm.2019.670	DNS
2022	243855360	10.1017/jfm.2022.749	DNS	2019	491520000	10.1017/jfm.2019.376	DNS
2022	268435456	10.1017/jfm.2022.402	DNS	2019	2147483648	10.1017/jfm.2018.1005	DNS
2022	12884901888	10.1017/jfm.2022.942	DNS	2019	210134016	10.1017/jfm.2019.787	DNS
2022	509607936	10.1017/jfm.2021.1080	DNS	2019	235376180	10.1017/jfm.2018.953	DNS
2022	3446016	10.1017/jfm.2022.587	DNS	2019	235929600	10.1017/jfm.2019.84	DNS
2022	3263299584	10.1017/jfm.2022.393	DNS	2019	75000000	10.1017/jfm.2019.179	DNS
2022	27917287424	10.1017/jfm.2022.574	DNS	2019	754974720	10.1017/jfm.2019.558	DNS
2022	280350720	10.1017/jfm.2022.456	DNS	2019	164167200	10.1017/jfm.2018.1000	DNS
2022	2828800000	10.1017/jfm.2022.80	DNS	2019	314572800	10.1017/jfm.2019.222	DNS
2022	4294967296	10.1017/jfm.2022.294	DNS	2019	884736000	10.1017/jfm.2019.995	DNS
2022	4194304	10.1017/jfm.2022.801	DNS	2019	12582912	10.1017/jfm.2019.100	DNS
2022	173232000	10.1017/jfm.2022.331	DNS	2018	33816576	10.1017/jfm.2018.242	DNS
2022	8053063680	10.1017/jfm.2022.699	DNS	2018	135075000	10.1017/jfm.2018.489	DNS
2022	38755584	10.1017/jfm.2021.1028	DNS	2018	11894784000	10.1017/jfm.2018.625	DNS
2021	707481600	10.1017/jfm.2021.827	DNS	2018	20966400	10.1017/jfm.2018.466	DNS
2021	150994944	10.1017/jfm.2021.814	DNS	2018	44160000	10.1017/jfm.2018.256	DNS
2021	93219840	10.1017/jfm.2021.524	DNS	2018	268435456	10.1017/jfm.2018.231	DNS
2021	1073741824	10.1017/jfm.2021.32	DNS	2018	83420000	10.1017/jfm.2018.503	DNS
2021	452984832	10.1017/jfm.2021.519	DNS	2018	92798976	10.1017/jfm.2018.408	DNS
2021	268435456	10.1017/jfm.2021.511	DNS	2018	16777216	10.1017/jfm.2018.389	DNS
2021	63606620160	10.1017/jfm.2021.231	DNS	2018	48500000	10.1017/jfm.2018.331	DNS
2021	39911040	10.1017/jfm.2021.448	DNS	2017	16777216	10.1017/jfm.2016.859	DNS
2021	1061683200	10.1017/jfm.2021.103	DNS	2017	1207959552	10.1017/jfm.2017.237	DNS
2021	16777216	10.1017/jfm.2021.757	DNS	2017	1944000000	10.1017/jfm.2017.53	DNS
2021	63700992	10.1017/jfm.2021.705	DNS	2017	152174592	10.1017/jfm.2017.372	DNS
2021	68719476736	10.1017/jfm.2021.288	DNS	2017	509607936	10.1017/jfm.2017.873	DNS
2021	554000000	10.1017/jfm.2021.312	DNS	2017	489715200	10.1017/jfm.2017.619	DNS
2021	192000000	10.1017/jfm.2021.535	DNS	2017	16777216	10.1017/jfm.2017.672	DNS
2021	2087321600	10.1017/jfm.2020.1144	DNS	2017	8000000	10.1017/jfm.2017.157	DNS
2021	1160000000	10.1017/jfm.2020.943	DNS	2017	408158208	10.1017/jfm.2017.398	DNS
2021	6039797760	10.1017/jfm.2020.913	DNS	2017	7077888	10.1017/jfm.2017.164	DNS
2020	134217728	10.1017/jfm.2020.159	DNS	2017	6879707136	10.1017/jfm.2017.371	DNS

Table 3: References used for the data points in Figure 1 (Part 2/3)

Year	Max Grid points	DOI	Type	Year	Max Grid points	DOI	Type
2017	11158866000	10.1017/jfm.2017.549	DNS	2010	12582912	10.1017/S0022112010000169	DNS
2016	8589934592	10.1017/jfm.2015.754	DNS	2010	650000	10.1017/S002211201000340X	DNS
2016	4186161	10.1017/jfm.2016.346	DNS	2010	35000000	10.1017/S002211200999423X	DNS
2016	4608000	10.1017/jfm.2016.554	DNS	2010	3227516928	10.1017/S0022112010003113	DNS
2016	536870912	10.1017/jfm.2016.207	DNS	2009	17921212416	10.1017/S0022112009007769	DNS
2016	752640000	10.1017/jfm.2016.179	DNS	2009	943936000	10.1017/S0022112009991388	DNS
2016	83886080	10.1017/jfm.2016.230	DNS	2009	149921280	10.1017/S0022112009992333	DNS
2015	131072000	10.1017/jfm.2015.9	DNS	2009	16777216	10.1017/S0022112008004916	DNS
2015	28459008	10.1017/jfm.2015.717	DNS	2009	7490265	10.1017/S0022112009007496	DNS
2015	120795955200	10.1017/jfm.2015.268	DNS	2009	17040384	10.1017/S0022112008004813	DNS
2015	14745600	10.1017/jfm.2015.566	DNS	2009	209715200	10.1017/S0022112009006624	DNS
2015	491206500	10.1017/jfm.2014.678	DNS	2009	6600000	10.1017/S0022112008005156	DNS
2015	327680000	10.1017/jfm.2015.696	DNS	2009	600000000	10.1017/S0022112008004473	DNS
2015	952247081	10.1017/jfm.2014.715	DNS	2008	4574147680	10.1017/S0022112008000864	DNS
2015	67108864	10.1017/jfm.2015.211	DNS	2008	622000000	10.1017/S0022112008001006	DNS
2014	11500000	10.1017/jfm.2014.589	DNS	2008	532480	10.1017/S0022112008004060	DNS
2014	9200000	10.1017/jfm.2014.368	DNS	2008	134217728	10.1017/S0022112007009883	DNS
2014	170393600	10.1017/jfm.2014.597	DNS	2008	106000000	10.1017/S0022112007009561	DNS
2014	78643200	10.1017/jfm.2014.68	DNS	2008	12880000	10.1017/S0022112008001985	DNS
2014	567730944	10.1017/jfm.2014.30	DNS	2008	98991585	10.1017/S0022112008000657	DNS
2013	262144000	10.1017/jfm.2012.596	DNS	2008	16777216	10.1017/S0022112008000141	DNS
2013	171884160	10.1017/jfm.2013.70	DNS	2008	629145600	10.1017/S0022112008002085	DNS
2013	3162112	10.1017/jfm.2013.361	DNS	2007	8589934592	10.1017/S0022112007008002	DNS
2013	67108864	10.1017/jfm.2013.130	DNS	2007	131995521	10.1017/S0022112007006192	DNS
2013	1153433600	10.1017/jfm.2013.142	DNS	2007	7807488	10.1017/S0022112007007380	DNS
2013	172800000	10.1017/jfm.2013.108	DNS	2007	12582912	10.1017/S0022112007004971	DNS
2012	268435456	10.1017/jfm.2012.59	DNS	2007	5270000	10.1017/S0022112007005836	DNS
2012	240000000	10.1017/jfm.2012.345	DNS	2007	3145728	10.1017/S0022112006004034	DNS
2012	134217728	10.1017/jfm.2012.241	DNS	2007	38707200	10.1017/S0022112007009020	DNS
2012	14495514624	10.1017/jfm.2012.428	DNS	2006	4227072	10.1017/S0022112006001121	DNS
2012	134217728	10.1017/jfm.2012.374	DNS	2006	2097152	10.1017/S0022112006001832	DNS
2012	373800960	10.1017/jfm.2012.400	DNS	2006	1179648	10.1017/S0022112006000711	DNS
2012	536870912	10.1017/jfm.2012.81	DNS	2006	93400000	10.1017/S002211200600262X	DNS
2012	1672704000	10.1017/jfm.2012.257	DNS	2006	1186816	10.1017/S0022112006002606	DNS
2011	134217728	10.1017/S0022112010005033	DNS	2005	251658240	10.1017/S0022112005006427	DNS
2011	2097152	10.1017/S0022112010005215	DNS	2005	1843200	10.1017/S0022112005003964	DNS
2011	78988950	10.1017/S0022112010005082	DNS	2005	5376000	10.1017/S0022112005003940	DNS
2011	6291456	10.1017/jfm.2011.219	DNS				
2011	26542080	10.1017/jfm.2011.252	DNS				
2011	28800000	10.1017/S0022112010005902	DNS				
2011	338000000	10.1017/S0022112010004866	DNS				
2011	211613535	10.1017/S0022112010005094	DNS				
2011	99186753	10.1017/jfm.2011.34	DNS				
2010	33600000	10.1017/S0022112010001278	DNS				
2010	944000000	10.1017/S002211201000039X	DNS				
2010	172800000	10.1017/S0022112010000893	DNS				
2010	84756225	10.1017/S0022112010003873	DNS				
2010	134217728	10.1017/S0022112010000807	DNS				
2010	252593991	10.1017/S0022112010001710	DNS				
2010	220000000	10.1017/S0022112010000558	DNS				

Table 4: References used for the data points in Figure 1 (Part 3/3)

Year	Max Grid points	DOI	Type	Year	Max Grid points	DOI	Type
2023	570000000	10.1017/jfm.2023.175	LES	2016	5782500	10.1017/jfm.2016.191	LES
2023	16777216	10.1017/jfm.2023.649	LES	2016	20480000	10.1017/jfm.2016.519	LES
2023	17039360	10.1017/jfm.2022.969	LES	2015	149760	10.1017/jfm.2015.29	LES
2023	30000000	10.1017/jfm.2023.331	LES	2015	4718592	10.1017/jfm.2015.604	LES
2023	12308967	10.1017/jfm.2023.575	LES	2015	134217728	10.1017/jfm.2015.249	LES
2023	19906560	10.1017/jfm.2023.499	LES	2015	134217728	10.1017/jfm.2015.116	LES
2023	38000000	10.1017/jfm.2023.143	LES	2014	452984832	10.1017/jfm.2014.381	LES
2022	184320	10.1017/jfm.2021.1156	LES	2014	1210056704	10.1017/jfm.2014.510	LES
2022	16777216	10.1017/jfm.2021.1150	LES	2014	6773760	10.1017/jfm.2014.379	LES
2022	840000000	10.1017/jfm.2022.692	LES	2014	4579600	10.1017/jfm.2014.581	LES
2022	3145728	10.1017/jfm.2022.577	LES	2014	40000000	10.1017/jfm.2014.505	LES
2022	1500000000	10.1017/jfm.2022.471	LES	2013	2097152	10.1017/jfm.2013.215	LES
2022	125000000	10.1017/jfm.2022.334	LES	2013	19300000	10.1017/jfm.2013.292	LES
2022	356352	10.1017/jfm.2022.654	LES	2013	10100000	10.1017/jfm.2013.135	LES
2022	31850496	10.1017/jfm.2021.1127	LES	2013	18874368	10.1017/jfm.2013.36	LES
2022	7200000	10.1017/jfm.2022.286	LES	2013	73711872	10.1017/jfm.2012.513	LES
2022	4047912960	10.1017/jfm.2021.1046	LES	2012	198656	10.1017/jfm.2012.84	LES
2021	11052800	10.1017/jfm.2021.4	LES	2012	16777216	10.1017/jfm.2012.115	LES
2021	4182410	10.1017/jfm.2021.332	LES	2012	150994944	10.1017/jfm.2012.73	LES
2021	40824000	10.1017/jfm.2021.261	LES	2012	1436506	10.1017/jfm.2011.539	LES
2021	10600000	10.1017/jfm.2021.1002	LES	2012	6553600	10.1017/jfm.2012.160	LES
2021	80621568	10.1017/jfm.2020.943	LES	2012	528384	10.1017/jfm.2012.150	LES
2021	712000000	10.1017/jfm.2021.714	LES	2011	6356992	10.1017/S0022112010005367	LES
2021	704643072	10.1017/jfm.2020.858	LES	2011	53248000	10.1017/jfm.2011.170	LES
2021	11291423	10.1017/jfm.2021.495	LES	2011	2097152	10.1017/jfm.2011.137	LES
2020	83886080	10.1017/jfm.2020.512	LES	2011	1800000	10.1017/S0022112011000450	LES
2020	134217728	10.1017/jfm.2020.622	LES	2011	25165824	10.1017/jfm.2011.342	LES
2020	8589934592	10.1017/jfm.2020.101	LES	2011	33554432	10.1017/S002211201000580X	LES
2020	201719808	10.1017/jfm.2020.536	LES	2011	25772032	10.1017/jfm.2011.130	LES
2020	80000000	10.1017/jfm.2019.711	LES	2010	4000000	10.1017/S0022112010000017	LES
2019	22118400	10.1017/jfm.2019.649	LES	2010	10616832	10.1017/S0022112010002995	LES
2019	16777216	10.1017/jfm.2018.910	LES	2010	43100000	10.1017/S0022112009992965	LES
2019	26000000	10.1017/jfm.2018.949	LES	2010	31843449	10.1017/S0022112010003927	LES
2019	27000000	10.1017/jfm.2019.80	LES	2010	1300000	10.1017/S0022112010000686	LES
2019	31997952	10.1017/jfm.2019.481	LES	2010	16777216	10.1017/S002211200999303X	LES
2019	134217728	10.1017/jfm.2019.591	LES	2009	2372500	10.1017/S0022112009006739	LES
2019	209715200	10.1017/jfm.2019.360	LES	2009	3538944	10.1017/S0022112009006867	LES
2019	294912	10.1017/jfm.2018.808	LES	2009	9208320	10.1017/S0022112008004722	LES
2019	327680	10.1017/jfm.2018.838	LES	2009	14515200	10.1017/S0022112009007277	LES
2018	100663296	10.1017/jfm.2018.644	LES	2009	134534400	10.1017/S0022112008005661	LES
2018	608000000	10.1017/jfm.2018.585	LES	2009	44346771	10.1017/S0022112009005801	LES
2018	400000000	10.1017/jfm.2018.470	LES	2008	25000000	10.1017/S0022112007009664	LES
2018	452984832	10.1017/jfm.2018.417	LES	2008	426951	10.1017/S0022112008003443	LES
2017	76800000	10.1017/jfm.2016.841	LES	2008	73728	10.1017/S0022112008001079	LES
2017	2147483648	10.1017/jfm.2017.172	LES	2007	1048576	10.1017/S002211200700599X	LES
2017	181000000	10.1017/jfm.2017.20	LES	2007	893952	10.1017/S0022112006004587	LES
2017	4500000000	10.1017/jfm.2017.187	LES	2007	20330271	10.1017/S0022112007006842	LES
2017	3145728	10.1017/jfm.2017.450	LES	2007	6000000	10.1017/S0022112006004502	LES
2016	2097152	10.1017/jfm.2015.744	LES	2007	32768	10.1017/S0022112007006155	LES
2016	262852998	10.1017/jfm.2016.628	LES	2007	11520000	10.1017/S002211200700897X	LES
2016	5782500	10.1017/jfm.2016.191	LES	2007	7000000	10.1017/S0022112006003235	LES
2016	20480000	10.1017/jfm.2016.519	LES	2006	18598932	10.1017/S0022112006000930	LES
2015	149760	10.1017/jfm.2015.29	LES	2006	50855936	10.1017/S0022112006009475	LES

- [16] Y. Yang, S. Qu, B. Cai, S. Liang, Z. Wang, J. Wang, and M. Xu, "Mapping global carbon footprint in china," *Nat. Comm.*, vol. 11, no. 1, p. 2237, 2020.
- [17] K. Lomas, M. Bell, S. Firth, K. Gaston, P. Goodman, J. R. Leake, A. Namdeo, M. Rylatt, D. Allinson, Z. Davies, *et al.*, "4M: measurement; modelling; mapping and management-the carbon footprint of uk cities," *ISOCARP Review*, vol. 6, 2010.
- [18] G. Bronevetsky, "Reliable high performance peta-and exa-scale computing," tech. rep., Lawrence Livermore National Lab.(LLNL), Livermore, CA (United States), 2012.
- [19] D. Kothe, S. Lee, and I. Qualters, "Exascale computing in the united states," *Comp. Sci. Eng.*, vol. 21, no. 1, pp. 17–29, 2018.
- [20] T. Tamura, "Towards practical use of LES in wind engineering," *J. Wind Eng. Ind. Aerod.*, vol. 96, no. 10-11, pp. 1451–1471, 2008.
- [21] D. Mehta, A. Van Zuijlen, B. Koren, J. Holierhoek, and H. Bijl, "Large eddy simulation of wind farm aerodynamics: A review," *J. Wind Eng. Ind. Aerod.*, vol. 133, pp. 1–17, 2014.
- [22] M. Abkar and F. Porté-Agel, "Influence of atmospheric stability on wind-turbine wakes: A large-eddy simulation study," *Phys. Fluids*, vol. 27, no. 3, p. 035104, 2015.
- [23] G. M. Starke, C. Meneveau, J. R. King, and D. F. Gayme, "The area localized coupled model for analytical mean flow prediction in arbitrary wind farm geometries," *Renew. Sust. Energ. Rev.*, vol. 13, no. 3, 2021.
- [24] C. R. Shapiro, J. Meyers, C. Meneveau, and D. F. Gayme, "Wind farms providing secondary frequency regulation: Evaluating the performance of model-based receding horizon control," *Wind Energy Sci.*, vol. 3, no. 1, pp. 11–24, 2018.
- [25] M. Abkar, A. Sharifi, and F. Porté-Agel, "Wake flow in a wind farm during a diurnal cycle," *J. Turbul.*, vol. 17, no. 4, pp. 420–441, 2016.
- [26] G. M. Starke, C. Meneveau, J. R. King, and D. F. Gayme, "A dynamic model of wind turbine yaw for active farm control," *Wind Energy*, pp. 1–17, 2023.
- [27] G. Narasimhan, D. F. Gayme, and C. Meneveau, "Effects of wind veer on a yawed wind turbine wake in atmospheric boundary layer flow," *Phys. Rev. Fluids*, vol. 7, no. 11, p. 114609, 2022.
- [28] F. Toja-Silva, T. Kono, C. Peralta, O. Lopez-Garcia, and J. Chen, "A review of computational fluid dynamics (CFD) simulations of the wind flow around buildings for urban wind energy exploitation," *J. Wind Eng. Ind. Aerod.*, vol. 180, pp. 66–87, 2018.
- [29] T. Mauery, J. Alonso, A. Cary, V. Lee, R. Malecki, D. Mavriplis, G. Medic, J. Schaefer, and J. Slotnick, "A guide for aircraft certification by analysis," tech. rep., NASA, 2021.
- [30] O. Lehmkuhl, G. Park, S. Bose, and P. Moin, "Large-eddy simulation of practical aeronautical flows at stall conditions," 2018.
- [31] K. A. Goc, P. Moin, S. T. Bose, and A. M. Clark, "Wind tunnel and grid resolution effects in large-eddy simulations of the high-lift common research model," *J. Aircraft*, pp. 1–13, 2023.
- [32] K. Goc, S. T. Bose, and P. Moin, "Large eddy simulation of the NASA high-lift common research model," in *AIAA SciTech 2022 Forum*, p. 1556, 2022.
- [33] K. A. Goc, O. Lehmkuhl, G. I. Park, S. T. Bose, and P. Moin, "Large eddy simulation of aircraft at affordable cost: a milestone in computational fluid dynamics," *Flow*, vol. 1, p. E14, 2021.
- [34] H. H. Xu, S. Lynch, and X. I. Yang, "Direct numerical simulation of slot film cooling downstream of misaligned plates," *Flow*, vol. 2, p. E7, 2022.
- [35] T. M. Corbett and K. A. Thole, "Large eddy simulations of kagome and body centered cubic lattice cells," *Int. J. Heat Mass Trans.*, vol. 218, p. 124808, 2024.

- [36] Y. Zhao and R. D. Sandberg, “High-fidelity simulations of a high-pressure turbine vane subject to large disturbances: Effect of exit mach number on losses,” *J. Turbomach.*, vol. 143, no. 9, p. 091002, 2021.
- [37] T. B. Kroll and K. Mahesh, “Large-eddy simulation of a ducted propeller in crashback,” *Flow*, vol. 2, p. E4, 2022.
- [38] N. Morse and K. Mahesh, “Tripping effects on model-scale studies of flow over the darpa suboff,” *J. Fluid Mech.*, vol. 975, p. A3, 2023.
- [39] M. Plasseraud, P. Kumar, and K. Mahesh, “Large-eddy simulation of tripping effects on the flow over a 6: 1 prolate spheroid at angle of attack,” *J. Fluid Mech.*, vol. 960, p. A3, 2023.
- [40] S. Altland, X. Zhu, S. McClain, R. Kunz, and X. Yang, “Flow in additively manufactured super-rough channels,” *Flow*, vol. 2, p. E19, 2022.
- [41] L. Lannelongue and M. Inouye, “Carbon footprint estimation for computational researchs,” *Nat. Rev. Methods Primers*, vol. 3, 2023.
- [42] H. S. Matthews, C. T. Hendrickson, and C. L. Weber, “The importance of carbon footprint estimation boundaries,” *Environ. Sci. Technol.*, vol. 42, no. 16, pp. 5839–5842, 2008.
- [43] A. Tukker, “Life cycle assessment as a tool in environmental impact assessment,” *Environ. Impact Assess. Rev.*, vol. 20, no. 4, pp. 435–456, 2000.
- [44] M. Z. Hauschild, R. K. Rosenbaum, and S. I. Olsen, *Life cycle assessment*. Springer, 2018.
- [45] D. W. Pennington, J. Potting, G. Finnveden, E. Lindeijer, O. Jolliet, T. Rydberg, and G. Rebitzer, “Life cycle assessment part 2: Current impact assessment practice,” *Environ. Int.*, vol. 30, no. 5, pp. 721–739, 2004.
- [46] M. Lee, N. Malaya, and R. D. Moser, “Petascale direct numerical simulation of turbulent channel flow on up to 786k cores,” in *Proceedings of the International Conference on High Performance Computing, Networking, Storage and Analysis*, pp. 1–11, 2013.
- [47] “Top 500.” <https://www.top500.org/>, 2023. Accessed: 01-29-2024.
- [48] C. Malone and C. Belady, “Metrics to characterize data center & it equipment energy use,” in *Proceedings of the Digital Power Forum, Richardson, TX*, vol. 35, sn, 2006.
- [49] T. G. Grid, “Green grid metrics: describing datacenter power efficiency: technical committee white paper,” 2007.
- [50] N. Lei and E. Masanet, “Climate-and technology-specific PUE and WUE estimations for US data centers using a hybrid statistical and thermodynamics-based approach,” *Resour. Conserv. Recy.*, vol. 182, p. 106323, 2022.
- [51] S. Greenberg, E. Mills, B. Tschudi, P. Rumsey, and B. Myatt, “Best practices for data centers: Lessons learned from benchmarking 22 data centers,” *Proceedings of the ACEEE summer study on energy efficiency in buildings in Asilomar, CA. ACEEE, August*, vol. 3, pp. 76–87, 2006.
- [52] J. Kaiser, J. Bean, T. Harvey, M. Patterson, and J. Winiecki, “Survey results: Data center economizer use,” *White Paper*, 2011.
- [53] D. Bizo, “Global PUEs — are they going anywhere?.” <https://journal.uptimeinstitute.com/global-pues-are-they-going-anywhere/>, 2023.
- [54] Office of Energy Statistics, U.S. Energy Information Administration, “Monthly Energy Review July 2023,” July 2023.
- [55] H. Ritchie, P. Rosado, and M. Roser, “Carbon intensity of electricity generation.” <https://ourworldindata.org/grapher/carbon-intensity-electricity>, 2023.
- [56] J. Jimenez and A. Pinelli, “The autonomous cycle of near-wall turbulence,” *J. Fluid Mech.*, vol. 389, p. 335–359, 1999.

- [57] X. Wu, P. Moin, J. M. Wallace, J. Skarda, A. Lozano-Durán, and J.-P. Hickey, “Transitional–turbulent spots and turbulent–turbulent spots in boundary layers,” *Proc. Natl. Acad. Sci. U.S.A.*, vol. 114, no. 27, pp. E5292–E5299, 2017.
- [58] X. I. A. Yang and A. Lozano-Durán, “A multifractal model for the momentum transfer process in wall-bounded flows,” *J. Fluid Mech.*, vol. 824, p. R2, 2017.
- [59] X. Chen, F. Hussain, and Z.-S. She, “Non-universal scaling transition of momentum cascade in wall turbulence,” *J. Fluid Mech.*, vol. 871, p. R2, 2019.
- [60] I. Marusic and J. P. Monty, “Attached eddy model of wall turbulence,” *Ann. Rev. Fluid Mech.*, vol. 51, no. 1, pp. 49–74, 2019.
- [61] X. I. Yang and C. Meneveau, “Hierarchical random additive model for wall-bounded flows at high reynolds numbers,” *Fluid Dyn. Res.*, vol. 51, no. 1, p. 011405, 2019.
- [62] X. I. Yang, S. Pirozzoli, and M. Abkar, “Scaling of velocity fluctuations in statistically unstable boundary-layer flows,” *J. Fluid Mech.*, vol. 886, p. A3, 2020.
- [63] X. I. Yang, J. Sadique, R. Mittal, and C. Meneveau, “Integral wall model for large eddy simulations of wall-bounded turbulent flows,” *Phys. Fluids*, vol. 27, no. 2, 2015.
- [64] M. Fowler, T. A. Zaki, and C. Meneveau, “A Lagrangian relaxation towards equilibrium wall model for large eddy simulation,” *J. Fluid Mech.*, vol. 934, p. A44, 2022.
- [65] A. Vadrot, X. I. Yang, and M. Abkar, “Survey of machine-learning wall models for large-eddy simulation,” *Phys. Rev. Fluids*, vol. 8, no. 6, p. 064603, 2023.
- [66] J. Kim, P. Moin, and R. Moser, “Turbulence statistics in fully developed channel flow at low reynolds number,” *J. Fluid Mech.*, vol. 177, pp. 133–166, 1987.
- [67] R. D. Moser, J. Kim, and N. N. Mansour, “Direct numerical simulation of turbulent channel flow up to $Re_\tau = 590$,” *Phys. Fluids*, vol. 11, pp. 943–945, 04 1999.
- [68] J. del Alamo, J. Jimenez, P. Zandonade, and R. MOSER, “Scaling of the energy spectra of turbulent channels,” *J. Fluid Mech.*, vol. 500, pp. 135–144, 2004.
- [69] S. Hoyas and J. Jiménez, “Scaling of the velocity fluctuations in turbulent channels up to $Re_\tau = 2003$,” *Phys. Fluids*, vol. 18, p. 011702, 01 2006.
- [70] M. Lee and R. D. Moser, “Direct numerical simulation of turbulent channel flow up to $Re_\tau = 5200$,” *J. Fluid Mech.*, vol. 774, p. 395–415, 2015.
- [71] M. Bernardini, S. Pirozzoli, and P. Orlandi, “Velocity statistics in turbulent channel flow up to $Re_\tau = 4000$,” *J. Fluid Mech.*, vol. 742, p. 171–191, 2014.
- [72] A. Lozano-Durán and J. Jiménez, “Effect of the computational domain on direct simulations of turbulent channels up to $Re_\tau = 4200$,” *Phys. Fluids*, vol. 26, p. 011702, 01 2014.
- [73] Y. Yamamoto and Y. Tsuji, “Numerical evidence of logarithmic regions in channel flow at $Re_\tau = 8000$,” *Phys. Rev. Fluids*, vol. 3, p. 012602, Jan 2018.
- [74] “Calculate your flight emissions.” https://co2.myclimate.org/en/flight_calculators/new, 2024. Accessed: 2024-01-29.
- [75] X. I. Yang and K. P. Griffin, “Grid-point and time-step requirements for direct numerical simulation and large-eddy simulation,” *Phys. Fluids*, vol. 33, no. 1, 2021.
- [76] J. Poore and T. Nemecek, “Reducing food’s environmental impacts through producers and consumers,” *Science*, vol. 360, no. 6392, pp. 987–992, 2018.

- [77] “Fossil co2 emissions per capita in the u.s.” <https://www.statista.com/statistics/1049662/fossil-us-carbon-dioxide-emissions-per-person/>. Accessed: 2024-02-03.
- [78] H. Choi and P. Moin, “Grid-point requirements for large eddy simulation: Chapman’s estimates revisited,” *Phys. Fluids*, vol. 24, no. 1, 2012.
- [79] Y. Li, E. Perlman, M. Wan, Y. Yang, C. Meneveau, R. Burns, S. Chen, A. Szalay, and G. Eyink, “A public turbulence database cluster and applications to study Lagrangian evolution of velocity increments in turbulence,” *J. Turbul.*, vol. 9, p. N31, 2008.
- [80] J. Graham, K. Kanov, X. Yang, M. Lee, N. Malaya, C. Lalescu, R. Burns, G. Eyink, A. Szalay, R. Moser, *et al.*, “A web services accessible database of turbulent channel flow and its use for testing a new integral wall model for les,” *J. Turbul.*, vol. 17, no. 2, pp. 181–215, 2016.
- [81] “Johns hopkins turbulence database.” <https://turbulence.pha.jhu.edu/>, 2024. Accessed: 2024-01-29.
- [82] P. R. Spalart and V. Venkatakrishnan, “On the role and challenges of CFD in the aerospace industry,” *Aeronaut.*, vol. 120, no. 1223, pp. 209–232, 2016.
- [83] M. Mani and A. J. Dorgan, “A perspective on the state of aerospace computational fluid dynamics technology,” *Ann. Rev. Fluid Mech.*, vol. 55, pp. 431–457, 2023.
- [84] F. T. Johnson, E. N. Tinoco, and N. J. Yu, “Thirty years of development and application of CFD at Boeing Commercial Airplanes, Seattle,” *Comput. Fluids*, vol. 34, no. 10, pp. 1115–1151, 2005.
- [85] P. Poisson-Quinton, “From wind tunnel to flight, the role of the laboratory in aerospace design,” *J. Aircraft*, vol. 5, no. 3, pp. 193–214, 1968.
- [86] S. Desai, “Relative roles of computational fluid dynamics and wind tunnel testing in the development of aircraft,” *Current Science*, vol. 84, no. 1, pp. 49–64, 2003.
- [87] “Wind tunnels and propulsion - boeing testing services.” <https://www.boeing.com/company/key-orgs/boeing-testing-services/wind-tunnels-and-propulsion#overview>. Accessed: 2024-02-03.
- [88] Federal Aviation Administration, “United States 2021 Aviation Climate Action Plan,” 2021.
- [89] M. Mofijur, S. F. Ahmed, Z. I. Rony, K. S. Khoo, A. A. Chowdhury, M. Kalam, I. A. Badruddin, T. Y. Khan, *et al.*, “Screening of non-edible (second-generation) feedstocks for the production of sustainable aviation fuel,” *Fuel*, vol. 331, p. 125879, 2023.
- [90] V. M. D. Pasa, C. A. Scaldaferrri, and H. dos Santos Oliveira, “Main feedstock for sustainable alternative fuels for aviation,” in *Sustainable Alternatives for Aviation Fuels*, pp. 69–102, Elsevier, 2022.